

## RESEARCH ARTICLE

# Investigation of the charging and discharging cycle in a thermal energy storage system

Dhruvil Panchigar<sup>1</sup>, Suchir Joshi<sup>2</sup>, Omkar Machindar<sup>3</sup>, Kaval Chapani<sup>4</sup>, Gursimran Singh<sup>5</sup>, Bibin B. S.<sup>6</sup>, Edison Gundabattini<sup>6\*</sup>

<sup>1</sup>IIT Kanpur, Kanpur, Uttar Pradesh, India 208016

<sup>2</sup>Friedrich-Alexander Universität Erlangen-Nürnberg 91054, Germany

<sup>3</sup>Department of Mechanical Engineering, FAU, Erlangen, 91052, Germany

<sup>4</sup>Materials Science and Technology, TU Bergakademie Freiberg, Freiberg-09599, Germany

<sup>5</sup>Bannerghatta Rd, Dollars Colony, 175-176c Phase 4, J. P. Nagar, Bengaluru, India 560076

<sup>6</sup>Department of Thermal and Energy Engineering, School of Mechanical Engineering, Vellore Institute of Technology, Vellore-632 014, India

**Abstract** – Phase change materials (PCMs) are the most suitable for storing thermal energy, as they store latent heat with a high storage energy density per unit volume. PCMs are a proven scheme of thermal management in the context of cooling electronic devices. This paper focuses on enhancing the efficiency as well as reducing the time during charging and discharging of the PCMs. Various aluminum fin structures in contact with PCM are analyzed using the finite volume method. Lauric acid-PCM is employed for the analysis in applications at low and mid-temperature ranges. The analysis was carried out with a 40 mm x 40 mm 2D vessel, a heat flux of 180 W/m<sup>2</sup> from the top surface, and a 3 mm-thick aluminum plate; the other sides are insulated with glass wool. Three cases are considered to contrast efficiency: vessels with no fins, vessels with 3 mm-diameter straight aluminum fins, and vessels with 1 mm-diameter periodic-structured aluminum fins (mesh fins) with a 10 mm cell base size. The three cases are analyzed in Ansys Fluent for charging time; the straight and periodic structured fins are also analyzed for discharging time. It was inferred from the results that vessels with straight fins had a 58% decrease in charging time as compared to vessels with no fins. Vessels with periodic structured fins had a 82% decrease in charging time as compared to vessels with no fins. Also, the periodic structured tubes required 61.5% less time to discharge than the straight tube structure. Hence, Periodic Structured fins and tubes could overcome the problem of a long time taken for charging and discharging PCM.

## Article History

Received : 27 June 2025

Revised : 28 August 2025

Accepted : 30 January 2026

Published : 15 March 2026

## Keywords

*Heat transfer fluid*

*Liquid fraction*

*Periodic structure*

*Phase change material*

*Thermal energy storage*

*Thermal profile*

## 1. Introduction

According to the Indian government, the country relies heavily on petroleum products for energy, which are being exhausted at a faster rate. Along these lines, for a sustainable future, it needs to consider other options. The researchers should focus more on cultivating renewable energy and storing it since the capacity of thermal energy is a significant necessity for ongoing events. All developing and developed countries make efforts to build efficient and structured thermal energy storage (TES) systems [1]. The major natural source of energy is the sun, which releases an enormous amount of energy. The sun is a limitless and pollution-free source of energy, which may be used to create energy-efficient solutions that minimize CO<sub>2</sub> emissions. The amount of solar energy falling on Earth exceeds our whole global energy supply of 13,800 Mtoe by a factor of ten [2]. There are several ways to store heat, including latent heat TES, packed-bed method, Aquifer TES, and pumped TES. The TES framework can hold and disseminate excellent heat for a more extended timeframe and through a more extended life expectancy [3]. Other than providing heat, heat storage is used for changing the heat into valuable energy [4]. The purpose of making energy plans is to teach, guide, and direct energy change measures. How they shape executives' organized sensemaking in the field is disregarded in the improvement of plans. The investigation follows the method involved in putting resources into a TES [5].

Thermal energy can be stored by sensible energy, latent energy, and thermochemical energy. Storage of thermal energy in the form of latent heat is more popular than the other two methods [6]. This is because it can achieve high storage energy density per unit volume, and these materials have high specific heat [7]. Phase change materials (PCMs) are useful to store latent heat energy because PCMs release nearly equal amounts of heat that are stored in the material during melting at a constant temperature. Based on this principle, many materials can fulfill the requirement, which are available in a wide range of inorganic salts to liquid metals [8]. Various materials are compared for high-temperature TES systems applications, out of which molten salts show the best properties for this application. The increase in Heat transfer is also evident to counter the weak heat transfer. So, the ideal materials to counter the problem are metal foams and graphite composites [9]. TES using nanoparticle-enhanced PCM in a shell-and-multitube unit was experimentally investigated at atmospheric pressure. Two distinct fatty acids and paraffin wax are utilized as the foundation for PCM. Nanoparticles are made of graphite and multi-walled carbon nanotubes [10].

Even paraffin is the most promising material for PCM. This is because, during the crystallization of the (CH<sub>3</sub>)-chain inside paraffin, a high value of latent heat will be released. With the increase in the number of carbon atoms, the latent

heat temperature of freezing and melting will also increase. Differential scanning calorimetry (DSC) analysis represents data of paraffin wax, such as latent heat, melting temperature, and specific heat [11]. Thermal storage (TES) is a potential technology for increasing energy efficiency. To utilize TES in future applications, there are still many areas that need to be improved, such as charging time, storage capacity, encapsulation of PCM, discharging, and many others. Because of its repeated usage feature, consistent heat source temperature, and high energy storage density, PCM has become a viable choice. PCM might be injected into supports such as bentonite, diatomite, expanded perlite, clay minerals, and vermiculite to create form-stable PCMs. Other PCMs that are acceptable for low-temperature heat storage systems (40-75 °C) require more investigation before they can be used in practice [12].

The use of PCMs in solar heating systems, energy conservation, textiles, thermal insulation, and air conditioning systems has gotten a lot of attention. Because of their flaws, such as the high-quality-cooling phenomena and phase separation, inorganic PCMs are restricted. Because organic PCMs leak quickly and have low thermal conductivity, better containment is required. An excellent latent heat storage material is an acidic fatty acid fused with expanded perlite (EP). It has a melting temperature of 33.0 °C and a latent heat of 131.3 kJ/kg, and the melting temperature and latent heat barely change after 1000 thermal cycles [13].

TES materials can keep thermal energy at an almost steady temperature. A few organic PCMs, such as alkanes, fatty acids, and their combinations, have been analyzed for heat storage applications. A few organic assisting materials that may release toxic gases include formaldehyde, which restricts their applications. The shape-stabilized lauric acid (LA) melts at 44.32 °C with a latent heat of 179.85 kJ/kg and solidifies at 41.72 °C. The LA served as a PCM for TES, while the activated carbon served as an adsorbent and support material. The shape stabilized LA with activated carbon composites melted at 44.07 °C with a latent heat of 65.14 kJ/kg and solidified at 42.83°C [14]. Recently, additive manufacturing has been employed for developing PCM-integrated components. A novel thermal buffering porous cube of nickel-titanium (PCNT) components was developed using this potential manufacturing technique. Because of their high latent heat and high thermal conductivity, these cubes have special TES capabilities. Under the right working fluid temperatures, PCNT's strong thermal conductivity and ability to withstand a reversible phase transition between austenite and martensite phases enable effective energy storage and release [15]. Further, a TES unit's performance was experimentally investigated using myristic acid (PCM) and water as the heat transfer fluid (HTF) at a low phase change temperature range of 53–55 °C [16], Figure 1.

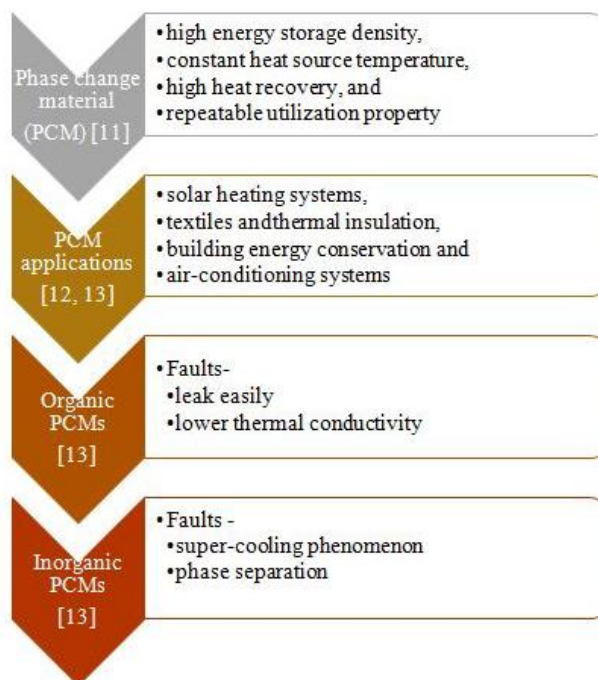


Figure 1. Phase change materials at a glance

Many experiments have been done on PCMs by changing the micro-structure, doping metallic nanoparticles, Multi-walled Carbon nanotube, carbon additives, graphene, and Graphite. Also, an experiment shows that the storage capacity of PCM and heat transfer rate can be increased by introducing a stepped fin inside it [17, 18], which eventually affects charging time. Additionally, recent investigations have shown that the fin-stone hybrid structure, which combines fins and natural stones, improves PCM heat transfer for TES applications. This structure has the benefits of being inexpensive, environmentally friendly, and easily accessible [19]. The primary factor is the encapsulating material and its thickness, which affects the heat transfer efficiency and enables the PCM to provide both flexibility and stability in terms of thermal and mechanical properties. Micro-encapsulation is highly favored for storage. The experiment was conducted by Behzad Maleki et al. [20], who covered PCM with CuO nano encapsulation, and the result showed that this will significantly affect storage capacity. The testing of PCM carried out on the scale model, by using the various non-dimensional numbers researched, derives valuable observations for the full-scale model [8]. A numerical simulation done by Ayoub Briache et

al. [21] indicated that copper nanoparticles enhanced PCM showed a meager improvement in the heat transfer coefficient. But metal foam with PCM showed an incredible performance by 12.3%. A qualitative experiment was done by Idris et al. [22] to determine the orientation of PCM to decide the lowest time possible to charge the storage, as shown in Figure 2. It was carried out experimentally by attaching thermocouples to the storage and using a CCD camera. Also, the computational fluid dynamics (CFD) analysis was done to check the temperature gradient of storage and charging time of storage in various storage positions, viz, at 0°, 45°, and 90°. A 2D CFD model for a shell and multi-tube energy storage was established and validated. The natural convection, liquid fraction distribution, and temperature rise were analyzed through the simulations. Various parameters, such as tube diameter, the eccentricity distance, and tube arrangement, were considered to investigate the thermal storage performance of the system [23]. In another TES application, PCM with various fin geometries, such as longitudinal fins and arc-shaped curved fins, is investigated. Results indicated significant performance of the PCM system [24]. Also, a twisted fin is incorporated in the PCM-based TES system. The system indicated a significant thermal performance with an average value 10.5% [25].

<b>PCM micro structure change</b> [8, 14, 15, 16, 21]	<b>PCM with stepped Fin, twisted Fin, curved Fin</b> [14, 15, 24, 25]	<b>PCM Orientation</b> [17]
<ul style="list-style-type: none"> <li>• doping metallic nanoparticles, carbon additives, Multi-walled Carbon nanotube, Graphite, and Graphene</li> <li>• increased storage capacity</li> </ul>	<ul style="list-style-type: none"> <li>• increased storage capacity</li> <li>• increased heat transfer rate</li> </ul>	<ul style="list-style-type: none"> <li>• lowest possible time to charge the storage</li> </ul>

Figure 2. Enhancing the rate of heat transfer of a PCM

A setup is designed by Jialin Yang et al. [26] to test the dynamic thermal behavior of a cylindrical latent heat thermal storage unit; their aim is to calculate the charging time with the variation of the material. Paraffin wax is used as PCM. Copper foam and a bottom fin are inserted into the PCM, and water is used as the HTF. Hence, under similar conditions, complete melting of PCM takes 33% faster than that of pure paraffin.

This paper has considered the cubical TES model and kept the vertical, constant heat flux of 180 W/m<sup>2</sup> provided through a metal plate on top. Under the same conditions of storage, numerical CFD simulations are done to simulate charging time by varying the fin configurations, such as vessels with no fins, vessels with 3 mm diameter straight aluminum fins and vessels with 1 mm diameter periodic structured aluminum fins (mesh fins) with 10 mm cell base size. Similarly, for discharging HTF passed through tubes under the action of gravity at a constant temperature of 300 K, through different tube structures.

## 2. Methodology

### 2.1 Geometry

Two-dimensional models were prepared to study the characteristics of charging and discharging of TES by Fusion 360. To compare charging characteristics, three models are shown in Figure 3. Model 1 is without a fin structure, Model 2 has straight fins, and Model 3 has periodic structured fins. These models have a porosity of 100%, 90% and 90% respectively. The size of the cavity is 40×40 mm, and the fins are inserted in the cavity. Porosity is defined as the ratio of the space occupied by PCM in the model to the available space of the model.

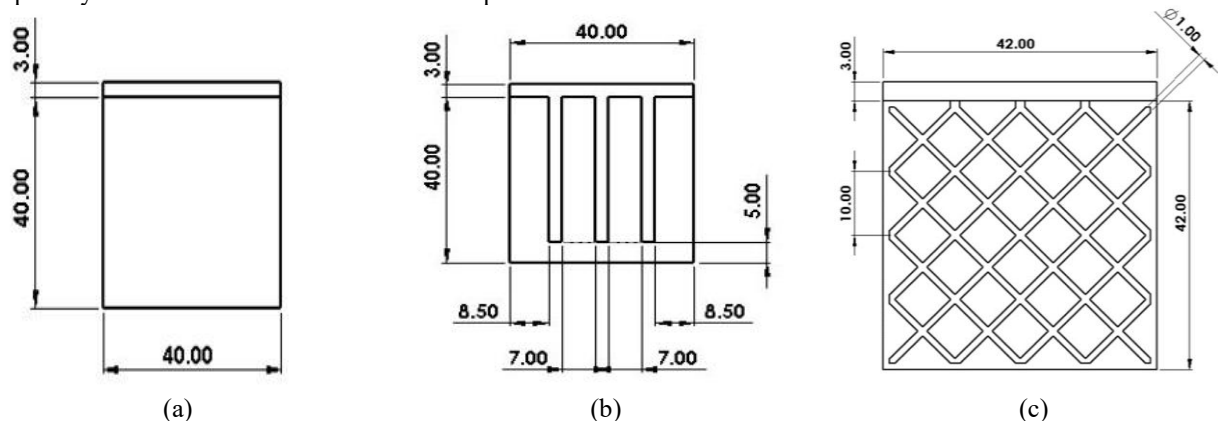


Figure 3. Geometry for charging (a) Model-1 (100% porosity), (b) Model-2 (90% porosity) and (c) Model-3 (90% porosity)

To analyze the discharge characteristic, models 4 and 5 were used (Figure 4). According to the previous studies, HTF passes from the reservoir at the top to the reservoir at the bottom through tubes, which pass through the PCM [27]. In the upper reservoir, HTF is kept at 300 K. Due to conduction, heat energy from PCM will pass to HTF. In model 4, the tube size is 2 mm, which is straight, whereas in model 5, the tubes are in a square mesh structure with a diameter of 1mm.

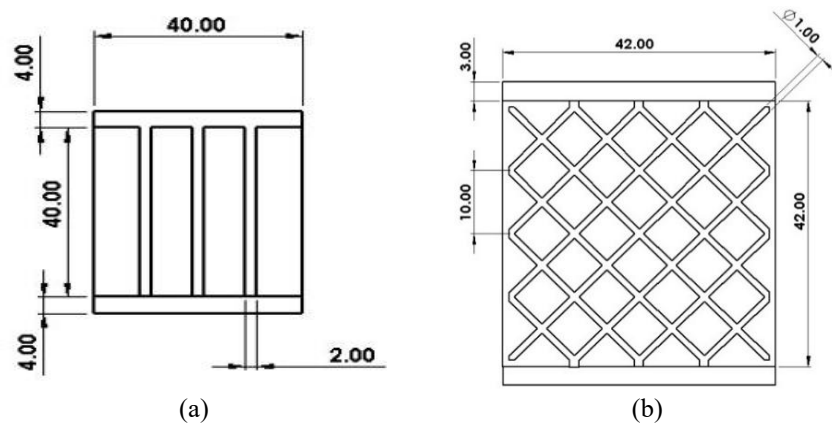


Figure 4. Geometry for discharging (a) model 4 (90% porosity) and (b) model 5 (90% porosity)

## 2.2 Material Properties

Lauric acid is used as PCM, whose thermo-physical properties are presented in Table 1. Since its solidus and liquidus temperatures are comparatively lower than those of other paraffin PCMs, this helps to reduce computation time during the transient simulation.

Table 1. Thermo-physical properties of Phase change material, [28]

Property	Value
Density	880 kg/m <sup>3</sup>
Specific heat capacity	2,300 J/kg K
Latent heat of fusion	1,87.2 kJ/kg
Melting temperature range	316.5 K (solidus) 321.7 K (liquidus)
Thermal conductivity	0.15 W/m K
Viscosity	11×10 <sup>-6</sup> m <sup>2</sup> /s

## 2.3 Meshing and Numerical Model

In a simulation to measure the charging and discharging time, the domain is divided into 41,000 quadrilateral elements, according to the grid independence test. The element size varied from 0.09 mm to 0.01 mm. The deviation in the result is negligible after 0.05 mm. Hence, an element size of 0.05 mm is taken for all simulations as shown in Figure 5.

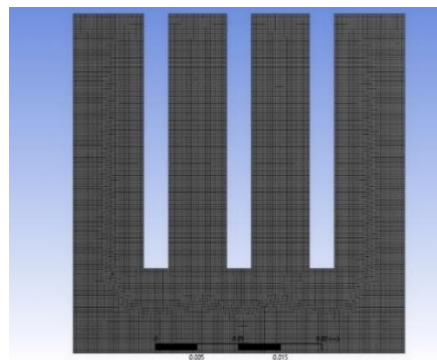


Figure 5. Meshed geometry (41000 elements)

Two-dimensional transient simulation done using ANSYS 2021 R1. ANSYS Fluent contains a built-in solidification/melting model, which is incorporated to simulate the melting and freezing conditions of PCM. The Enthalpy-porosity method is used for modeling the process of melting PCM in the latent heat TES, with a fixed grid.

The viscous-laminar model and solidification/melting model are incorporated for the simulation of PCM charging and discharging cycles. While defining the material properties of PCM, the Boussinesq approximation is invoked to define constant density and to consider natural convection. Because of the small temperature change during the process, there will be less heat transferred to the material, hence the change in density of the material is less than 1%. Under this given condition, the Boussinesq approximation is to be implemented [29].

### 2.4 Governing Equation

During the charging of TES, heat transfer from the metal to PCM occurs through the conduction mode of heat transfer. The equation used for the simulation of square geometry was the general equation for heat conduction, with constant PCM property. There was no internal heat generation. The equation is:

$$\rho_{PCM} \cdot c_{p,PCM} \cdot \frac{\partial T}{\partial t} = \frac{\partial}{\partial x} \left( k_{PCM} \cdot \frac{\partial T}{\partial x} \right) + \frac{\partial}{\partial y} \left( k_{PCM} \cdot \frac{\partial T}{\partial y} \right) + \frac{\partial}{\partial z} \left( k_{PCM} \cdot \frac{\partial T}{\partial z} \right) \tag{1}$$

For discharging, the TES system is split into 3 parts: PCM, HTF, and the tube. During discharge of TES, heat transfer is done by convection and conduction mode of heat transfer. The equation for heat conducted from PCM to the tube is given by Eq. (2) [21]:

$$\rho_T \cdot C_{p,T} \cdot \frac{\partial T}{\partial t} = \frac{1}{r} \frac{\partial}{\partial r} \left( k_T \cdot r \cdot \frac{\partial T}{\partial r} \right) + \frac{\partial}{\partial z} \left( k_T \cdot \frac{\partial T}{\partial z} \right) \tag{2}$$

For heat convection between the tube encapsulation tube and HTF, expressed as shown by Eq. (3) [17]:

$$\rho \cdot C_p \left( \frac{\partial T}{\partial t} + v_r \cdot \frac{\partial T}{\partial r} + v_z \cdot \frac{\partial T}{\partial z} \right) = k \left[ \frac{1}{r} \frac{\partial}{\partial r} \left( r \cdot \frac{\partial T}{\partial r} \right) + \frac{\partial^2 T}{\partial z^2} \right] \tag{3}$$

where  $\rho$  is the density,  $C_p$  is the specific heat capacity,  $k$  is the thermal conductivity, and  $T$  is the temperature.

### 2.5 Mushy Zone Constant

Mushy zone constant ( $A_{mush}$ ) is the crucial parameter while simulating the solidification and melting process, since there will be natural convection present within the PCM. With the high  $A_{mush}$  constant, the material turns to fluid quickly, which reduces heat convection through the melt region, hence delaying the melting observed, while the lower  $A_{mush}$  value will increase the heat convection. The effect of the mush constant was predominantly observed during the solidification. ANSYS Fluent provides a mushy zone constant range from 105 to 107 [30]. It is important to opt for the proper mushy zone constant for an accurate result. The optimum Mushy Zone constant, which is 106, was selected for the present analysis. According to various experiments,  $A_{mush}$  is constant for the different simulated conditions for lauric acid, Table 2 [31].

Table 2.  $A_{mush}$  constant for the different simulating conditions for lauric acid, [31, 32]

PCM	$A_{mush}$ (kg/(m <sup>3</sup> s))	$T_m$ (K)	Vessel shape
Lauric acid	316.65 - 321.35	106	Rectangular with vertical fins
Lauric acid	316.65-321.35	108	Square with metal foam
Lauric acid	316.65-321.35	5 *10 <sup>6</sup>	Rectangular

### 2.6 Simulation Parameters

The simulation parameters used for charging and discharge cycles are presented in Tables 3 and 4, respectively. During discharge of TES, the temperature rise of HTF is negligible. Hence, the initial temperature of all tube walls was kept similar to water at 300 K. A pressure-velocity coupled SIMPLE scheme with second-order upwind discretization for energy and momentum was incorporated for better accuracy.

Table 3. Simulation parameters for charging of TES

Phase change material	Lauric acid
PCM initial temperature	300 K
Fin material	Aluminium
Heat flux from fins	180 W/m <sup>2</sup>
Heat flux at the wall	0 W/m <sup>2</sup>

Table 4. Simulation parameters for the discharging of TES

Phase change material	Lauric acid
PCM initial temperature	340 K
Heat transfer fluid (HTF)	water
HTF temperature	300 K
Heat flux at the wall	0 W/m <sup>2</sup>

## 3. Results and Discussions

### 3.1 Charging of Thermal Energy Storage

To simulate the charging process, the models were assumed to be enclosed and adiabatic. The heat flux through the aluminum fin is 180 W/m<sup>2</sup> at steady-state conditions. From the result, it is observed that with the use of a fin, heat can transfer directly to the inner region of PCM (Figure 6). Investigation indicates that, compared to model 1, in models 2

and 3, the volume average temperature at the same time is higher. Furthermore, the volume-averaged temperature of module 3 is more than that of model 2, because heat transfer to the PCM is more uniform in model 3. The effect of it will be experienced on the liquid fraction. Hence, the liquid fraction will be highest for model 3 at any time instance, followed by model 2 and model 1, as shown in Figure 6.

Since heat energy reaches directly into the core of PCM through fins instead of natural convection through the Mushy region, the volume-averaged liquid fraction will increase, as shown in Figure 7. From Figure 8, it is confirmed that for model 3, at a time of 1250 seconds, lauric acid is going through the phase change and its temperature is 315 K, which is nearer to its solidus temperature (314 K). Table 5 represents data from the simulation, which shows that model 3 gets the first melting point at a time of 1175 seconds, and the volume average temperature is at 315K, which is closer to lauric acid liquidous temperature. Hence, it is concluded that using a periodic fin structure transmits heat uniformly in all regions. This helped to achieve the lowest charging time. Whereas in model 1, heat is provided from only the top, due to the lower conductivity of PCM, the TES charging time is the highest.

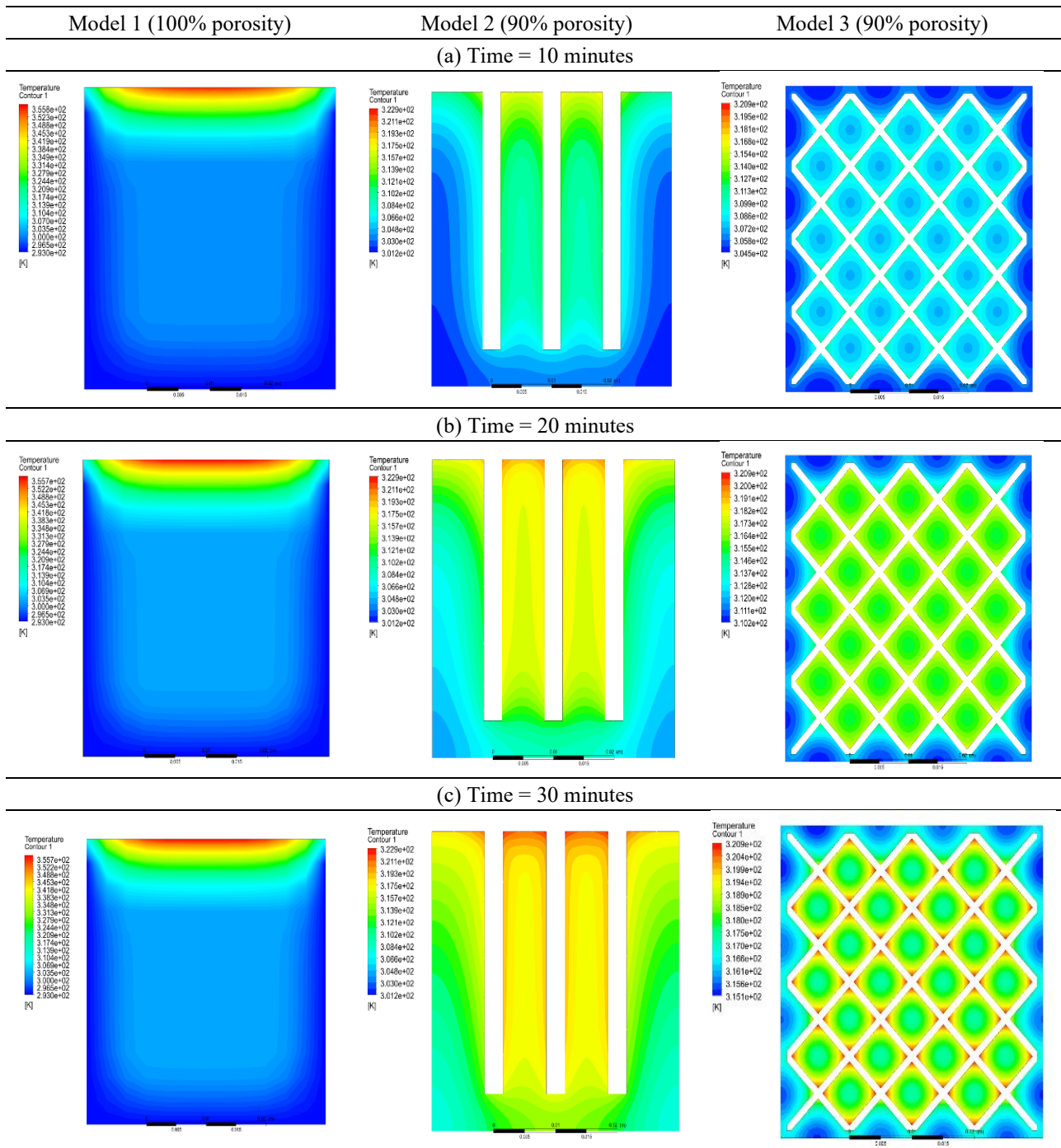


Figure 6. Thermal profile (charging) in models 1, 2 and 3

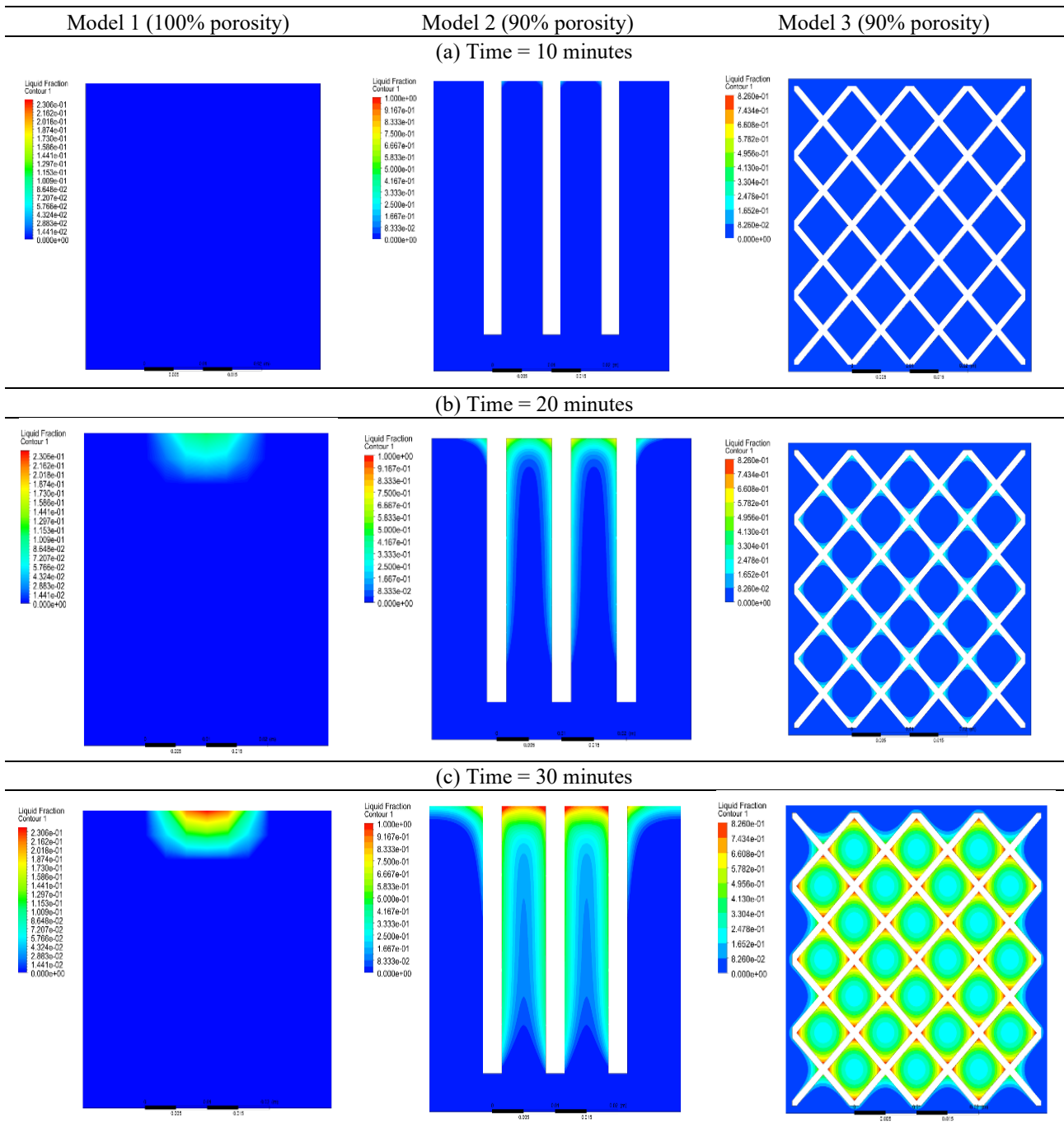


Figure 7. Thermal profile (discharging) of PCMs in models 1, 2 and 3

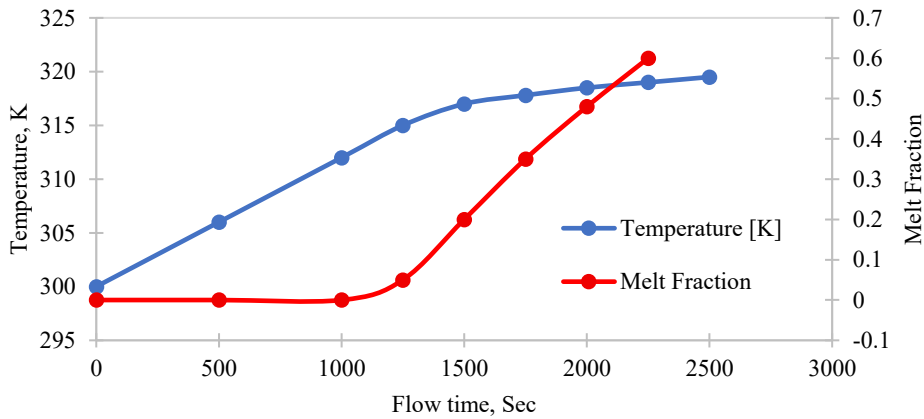


Figure 8. Volume-averaged liquid fraction and temperature with time (model 3)

Table 5. Charging time comparison

	First melting point Time, Sec	Volume Averaged Temperature, K	Volume-averaged liquid fraction line slope	Expected total melting time, Sec
Model 1	2200	305	0.000006	18866
Model 2	1250	310	0.000155	7916
Model 3	1175	315	0.000455	3397

### 3.2 Discharging of Thermal Energy Storage and Validation

To simulate the discharge process, water as HTF passed through tubes at 300 K, driven by gravity. The PCM was kept at 340 K, which is above the liquidus temperature. As observed in Figure 9, the use of periodic structured tubes to carry HTF will absorb heat uniformly from the whole PCM volume. Hence, discharge will be complete in 250 seconds, which can be concluded. For solidification, the mushy zone shows the predominant effect; it is observed that the % of mushy zone volume with respect to total volume, in model 5, is less than in model 4. It is the reason behind the fast heat transformation.

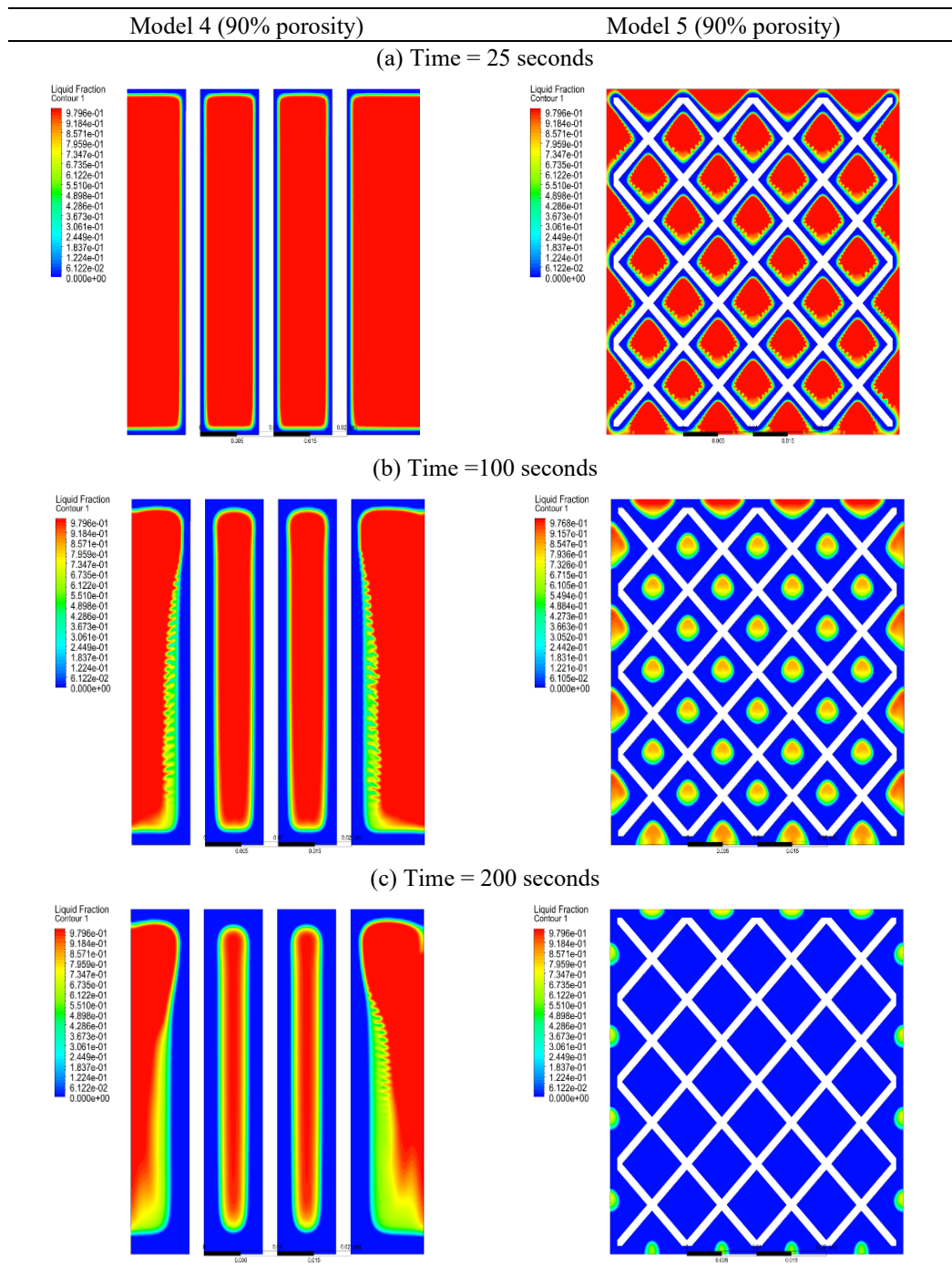


Figure 9. Heat transfer through periodic structured tubes

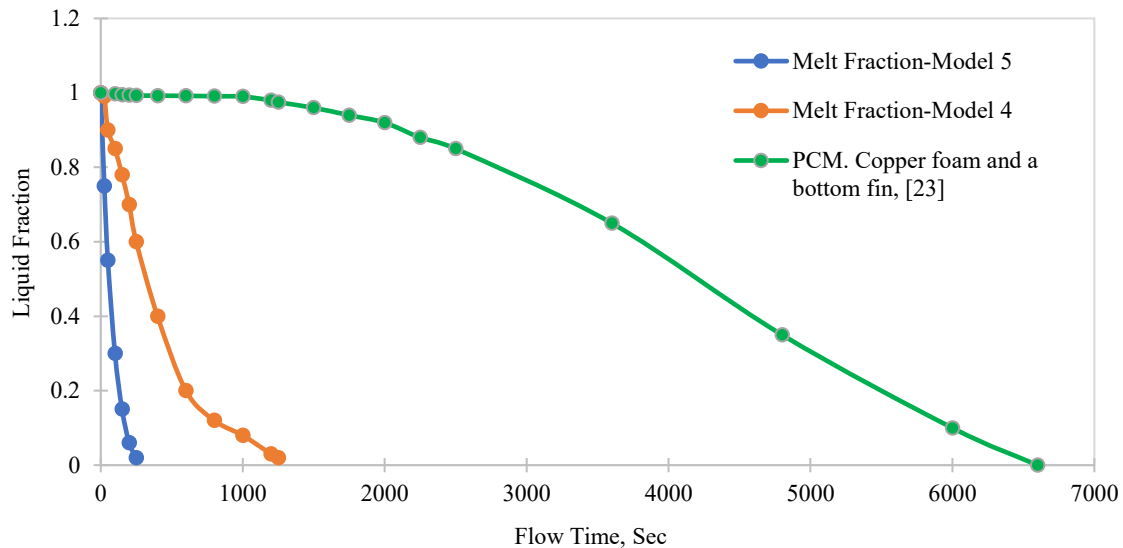


Figure 10. Volume-averaged liquid fraction while discharging

From Table 6, it is indicated that the complete discharge of TES of model 5 will be complete in 250 seconds, whereas in model 4, at 1000 seconds, 10 % liquid remains to convert into solid. Results indicated that the discharging rate will be faster in the periodic structured tube model (model 5) compared to the straight tube model (model 4), and the discharging time is reduced by 400% for solidification of the same amount of PCM under similar conditions, Figure 10. The reduction in the charging and discharging time helps to store energy faster and more easily. The results of the two models, 4 and 5, that were investigated are compared with the published literature. Results revealed that the melt fraction model 5 (periodic structured tube setup) with 90% porosity is 2500% faster than the PCM copper foam and a bottom fin arrangement. Hence, the present work is validated and proves the best bet in charging and discharging time of the PCMs.

Table 6. Discharging time comparison

	Discharging time, Sec	Volume-averaged liquid fraction
Model 4	650	0.2 (at 600sec)
Model 5	250	0.0 (at 250 sec)
PCM copper foam and a bottom fin, [23]	6600	0.0 (at 6600 sec)

#### 4. Conclusion

To simulate the discharging process, similar tube setups are used, such as the straight-tube model and the periodic-structured tube model. These tubes are immersed in melt PCM, and water at 300 K is passed through the tubes in both models. According to the simulation results, charging PCM with straight fins and periodic structured fins is compared with charging PCM without fins. It is observed that as the surface-to-volume ratio increases, melting will start earlier, and charging time decreases significantly. The fins will distribute heat uniformly throughout the structure, thereby reducing the maximum charging time by 81%. The results indicate that discharge will be faster with the periodic structured tube setup than with a straight-through tube setup. As the surface-to-volume ratio increases, heat transfer from PCM to HTF becomes more uniform, leading to a decrease in discharge time. The simulation shows that using a periodic structure tube setup reduces the discharging time by more than 60%.

The simulation results show that as the surface-to-volume ratio increases, charging time decreases. So, an increase in surface roughness will also support reducing charging time. Improving the thermal properties of PCM by adding nanoparticles will help reduce charging and discharging time. The tube material that carries HTF will also affect the discharge time. The above-discussed TES methods have excellent storage capacity and efficiency, which can be further improved by making appropriate modifications. Further experimental and numerical investigations are needed to enable TES for everyday use. Moving towards renewable energy can surely save our environment and provide a sustainable future.

#### Conflict of Interest Statement

Regarding this study, the authors disclose no conflicts of interest. We promise to promptly disclose any potential conflicts of interest that may come up during the evaluation process.

#### Authors Contribution

Dhruvil Panchigar (Conceptualisation; Methodology; Data curation; Investigation; Software; Visualisation; Writing - original draft)

Suchir Joshi Omkar Machindar (Conceptualisation; Methodology; Data curation; Investigation; Software; Visualisation; Writing - original draft)  
 Kaval Chapani (Conceptualisation; Methodology; Data curation; Investigation; Software; Visualisation; Writing - original draft)  
 Gursimran Singh (Conceptualisation; Methodology; Data curation; Investigation; Software; Visualisation; Writing - original draft)  
 Bibin B. S (Conceptualisation; Methodology; Validation; Writing - review & editing)  
 Edison Gundabattini (Conceptualisation; Methodology; Validation; Writing - review & editing; Supervision)

### Acknowledgments

The authors are grateful to the management of the Vellore Institute of Technology (VIT) for their continual support.

### Funding

This research did not obtain any explicit grant from agencies in the public, commercial, or not-for-profit sectors.

### Reference

- [1] A. Nandi, N. Biswas, "Melting dynamics and energy efficiency of nano-enhanced phase change material (NePCM) with graphene, Al<sub>2</sub>O<sub>3</sub>, and CuO for superior thermal energy storage (TES)," *Journal of Energy Storage*, vol. 109, p. 115076, 2025.
- [2] L. Seyitini, B. Belgasim, C.C. Enweremadu, "Numerical investigation of a hybrid latent-sensible thermal energy storage system for low temperature industrial applications," *Journal of Energy Storage*, vol. 123, p. 116759, 2025.
- [3] K. Vigneshwaran, G. Singh Sodhi, P. Muthukumar, S. Subbiah, "Concrete based high temperature thermal energy storage system: Experimental and numerical studies," *Energy Conversion and Management*, vol. 198, p. 111905, 2019.
- [4] T. Christen, "Ragone plots and discharge efficiency-power relations of electric and thermal energy storage devices," *Journal of Energy Storage*, vol. 27, p. 101084, 2020.
- [5] N. Bertelsen, M. Caussarieu, U. R. Petersen, P. Karnøe, "Energy plans in practice: The making of thermal energy storage in urban Denmark," *Energy Research & Social Science*, vol. 79, p. 102178, 2021.
- [6] H. Jouhara, A. Żabnieńska-Góra, N. Khordehghah, D. Ahmad, T. Lipinski, "Latent thermal energy storage technologies and applications: A review," *International Journal of Thermofluids*, vol. 5, p. 100039, 2020.
- [7] L. F. Cabeza, *Advances in Thermal Energy Storage Systems: Methods and Applications*. Cambridge, MA, USA: Woodhead Publishing (Elsevier), 2021.
- [8] K. Kant, A. Shukla, A. Sharma, "Advancement in phase change materials for thermal energy storage applications," *Solar Energy Materials and Solar Cells*, vol. 172, pp. 82–92, 2017.
- [9] H. Wang, J. Liu, Y. Wang, Y. Zhao, G. Zhang, "A review of the performance and application of molten salt-based phase change materials in sustainable thermal energy storage at medium and high temperatures," *Applied Energy*, vol. 389, p. 125766, 2025.
- [10] M. Fabrykiewicz, J.T. Cieśliński, "Experimental investigation of thermal energy storage in shell-and-multi-tube unit with nano-enhanced phase change material," *Applied Thermal Engineering*, vol. 246, p. 122881, 2024.
- [11] A. Agarwal, R. M. Sarviya, "Characterization of commercial grade paraffin wax as latent heat storage material for solar dryers," *Materials Today: Proceedings*, vol. 4, no. 2, pp. 779–789, 2017.
- [12] Q. Shen, J. Ouyang, Y. Zhang, H. Yang, "Lauric acid/modified sepiolite composite as a form-stable phase change material for thermal energy storage," *Applied Clay Science*, vol. 146, pp. 14–22, 2017.
- [13] X. Liu, Y. Zhao, Z. Fan, Y. Shi, D. Jiang, "Preparation and characterization of lauric acid–stearic acid/expanded perlite as a composite phase change material," *RSC Advances*, vol. 12, no. 37, pp. 23860–23868, 2022.
- [14] Y. Chen, G.E. Minrong, Z. Feng, Y. Xue, "Synthesis of lauric-myristic acid/activated carbon composite as a new shape-stabilized energy storage material," *Medziagotyra*, vol. 28, no. 1, pp. 68–74, 2022.
- [15] A.A. Wilson, M. Ozsipahi, M.C. Fish, D.J. Sharar, A. Bayba, I. Karaman et al., "High power thermal energy storage from ordered-pore additively manufactured phase-transforming nickel-titanium porous cubes," in *Proceedings of the 23rd IEEE Intersociety Conference on Thermal and Thermomechanical Phenomena in Electronic Systems (ITherm)*, Aurora, CO, USA, 2024, pp. 1–8.
- [16] A. Surya, R. Prakash, N. Nallusamy, "Experimental study on the charging and discharging performance of a thermal energy storage unit using low temperature phase change material," *Journal of Energy Storage*, vol. 103, p. 114311, 2024.
- [17] P.M. Kumar, D. Sudarvizhi, P.M.J. Stalin, A. Aarif, R. Abhinandhana, A. Renuprasanth et al., "Thermal characteristics analysis of a phase change material under the influence of nanoparticles," *Materials Today: Proceedings*, vol. 45, pp. 7876–7880, 2021.
- [18] M. E. Nakhchi, J. A. Esfahani, "Improving the melting performance of PCM thermal energy storage with novel stepped fins," *Journal of Energy Storage*, vol. 30, p. 101424, 2020.
- [19] S. Zhang, Y. Yan, Z. Cheng, F. Wang, "Charging and discharging in thermal energy storage unit with fin-stone hybrid structure for enhancing heat transfer of phase change materials," *International Journal of Heat and Mass Transfer*, vol. 224, p. 125325, 2024.
- [20] B. Maleki, A. Khadang, H. Maddah, M. Alizadeh, A. Kazemian, H. M. Ali, "Development and thermal performance of nanoencapsulated PCM/ plaster wallboard for thermal energy storage in buildings," *Journal of Building Engineering*, vol. 32, p. 101727, 2020.
- [21] A. Briache, A. Afass, M. Ouardouz, M. Ahachad, M. Mahdaoui, "A comparative analysis of enhancement techniques in a PCM-embedded heat sink: Fin forms, nanoparticles, and metal foam," *International Journal of Heat and Mass Transfer*, vol. 229, pp. 125730–125730, 2024.
- [22] I. Al Siyabi, S. Khanna, T. Mallick, S. Sundaram, "An experimental and numerical study on the effect of inclination angle of phase change materials thermal energy storage system," *Journal of Energy Storage*, vol. 23, pp. 57–68, 2019.
- [23] M. Chen, Y. Si, L. Ma, C. Zhu, P. Li, "Simulation of performance optimization of a latent heat thermal energy storage device," in *2024 7th International Conference on Power and Energy Applications (ICPEA)*, Taiyuan, China, 2024, pp. 576–581.

- [24] S.A. Khan, H. Liu, H.E. Abdellatif, Z. Wang, A. Belaadi, A. Alhushaybari, "Investigation on enhancing thermal energy storage performance of a phase change material in triplex tube heat exchangers with novel fins configuration." *International Communications in Heat and Mass Transfer*, vol. 167, p. 109265, 2025.
- [25] P. Ding, Q. Ji, Y. Zou, "Enhancing the efficiency of latent heat thermal energy storage units with twisted fin induced natural convection." *International Journal of Thermal Sciences*, vol. 214, p. 109842, 2025.
- [26] J. Yang, L. Yang, C. Xu, X. Du, "Experimental study on enhancement of thermal energy storage with phase-change material," *Applied Energy*, vol. 169, pp. 164–176, 2016.
- [27] M. Cascetta, G. Cau, P. Puddu, F. Serra, "A comparison between CFD simulation and experimental investigation of a packed-bed thermal energy storage system," *Applied Thermal Engineering*, vol. 98, pp. 1263–1272, 2016.
- [28] A. Gautam and R. P. Saini, "A review on technical, applications and economic aspect of packed bed solar thermal energy storage system," *Journal of Energy Storage*, vol. 27, p. 101046, 2020.
- [29] P. Fleuchaus, B. Godschalk, I. Stober, P. Blum, "Worldwide application of aquifer thermal energy storage – A review," *Renewable and Sustainable Energy Reviews*, vol. 94, pp. 861–876, 2018.
- [30] A. Giovannelli, M. A. Bashir, "Charge and discharge analyses of a PCM storage system integrated in a high-temperature solar receiver," *Energies*, vol. 10, no. 12, pp. 1–13, 2017.
- [32] A. C. Kheirabadi and D. Groulx, "The effect of the mushy-zone constant on simulated phase change heat transfer," in *Proceedings of the 6th International Symposium on Advances in Computational Heat Transfer (CHT-15)*, New Brunswick, NJ, USA, May 2015, pp. 528–549.

## Nomenclature

### Abbreviations

PCM	Phase Change Material
CFD	Computational Fluid Dynamics
TES	Thermal energy storage
DSC	Differential Scanning Calorimetry
EP	Expanded perlite
HTF	Heat Transfer Fluid
LA	Lauric acid

### Symbols

$\rho$	Density
$c_p$	Specific Heat
$k$	Thermal conductivity

### Subscript

T	Tube
---	------